

ELECTRON SPECTROSCOPY OF CdMeTe NANOSTRUCTURES CREATED ON CdTe SURFACE UNDER ION BOMBARDMENT

Ergashov Yokub^{1,*}, and Umirzakov Boltakhodja¹

¹Tashkent State Technical University, 100095, 2-University street, Tashkent, Uzbekistan

Abstract. The electronic structure of CdMeTe nanostructures was studied by a variety of techniques of secondary and photoelectron spectroscopy. Particularly, for the first time it has been shown that in the conductivity band of the CdZnTe films there are maximums peaks of free electronic states with energies 3.5 and 4.4 eV relative E_v .

1 Introduction

Multi-layer thin-film structures based on semiconductor compounds A^2B^6 are widely used to design diverse optoelectronic devices, including solar cells. We have investigated crystalline structure of CdTe, CdZnTe and HgCdTe films, as well as their optical properties and how they change under different influences [1-6]. It was shown that properties of these films mainly depend on a synthesis technique, on their thickness and properties of a near-contact (transitive) layer formed on the boundary film-substrate. In recent years a techniques of low-energy ion implantation is frequently used for nano-sized structures on the surface and in near-surface region of semiconductor and dielectric films [7-10]. Particularly, the films of $Cd_{0.5}Ba_{0.5}Te$ were produced by the Ba^+ ion implantation into CdTe in combination with annealing [10]. It was established that the state densities of valence electrons and the forbidden band width of the CdBaTe nanofilms for $d \leq 25-30 \text{ \AA}$ depend on film thickness.

This paper reports the energy band parameters and the results of the study of the density of electronic states in the valence band and in the conductivity band for three-component nanofilms of $Cd_{1-x}Me_xTe$ produced by Ba and Zn ion implantation into CdTe.

2 Experimental methods

Single crystalline CdTe(100) of the n-type with the sizes $10 \times 10 \times 1 \text{ mm}^3$ were polished and treated with an etchant. The investigation was carried out in vacuum (10^{-6} bar) by Auger-electron spectroscopy (AES), ultraviolet photoelectron spectroscopy (UPS), electron energy loss spectroscopy (EELS) and by measurements of energy dependencies of the coefficients of secondary electron emission (SEE) and intensities of light transmitting through the sample. Morphology and degree of surface roughness were studied by scanning electron microscopy (SEM) and atomic force microscopy (AFM). The profiles of atom distributions in depth were defined by AES in combination with ion etching. Ion bombardment was made perpendicular to the target surface under vacuum (10^{-6} bar). Before ion implantation the CdTe samples were degassed by heating up to $T=1100 \text{ K}$ in combination with mild etching with the Ar^+ ions under vacuum (10^{-7} bar). By varying energy of the Ba^+ and Zn^+ ions within the range 0.5-5 keV the three-component nanoscale structures with the thickness 20-50 nm were produced. The optimal modes of ion implantation and annealing for the nanocrystals (NC) and nanofilms (NF) of CdMeTe/CdTe(100) are presented in Table 1.

Table 1. Optimal modes of formation of three-component nanostructures of CdMeTe/CdTe (100).

Ions	E_0 , keV	D , cm^{-2}	T_0 , K	Structure	Approximate composition	Film thickness, \AA
Ba	1	10^{15}	900	NC	$Cd_{0.6}Ba_{0.4}Te$	35-40
		$6 \cdot 10^{16}$	1000	NF	$Cd_{0.5}Ba_{0.5}Te$	35-40
	3	10^{15}	900	NC	$Cd_{0.7}Ba_{0.3}Te$	50-60
		$8 \cdot 10^{16}$	1000	NF	$Cd_{0.5}Ba_{0.5}Te$	50-60
Zn	1	10^{15}	850	NC	$Cd_{0.6}Zn_{0.4}Te$	40-45
	1	$8 \cdot 10^{16}$	800	NF	$Cd_{0.7}Zn_{0.3}Te$	-

* Corresponding author: vergashev@rambler.ru

3 Results and discussion

The photoelectron spectra of pure CdTe(100) and CdTe(100) with the Cd_{0.6}Zn_{0.4}Te film which were measured for $h\nu=10.8$ eV are presented in Fig.1. The spectral structure, i.e. the density of valence electron states of matrix and film, greatly differ from each other. The peaks corresponding to E_1 , E_2 and E_3 in the CdTe spectrum can be associated with hybridization of the 5p and 5s electrons of Te with the 5s and 4d ones of Cd. In the case of a three-component film, along with the Cd and Te electrons the 3d and 4s electrons of Zn will participate in electron hybridization owing to which the re-distribution of the density of valence electron states takes place. Besides these peaks, in the spectra there are peaks associated with the surface states (E_{ss}) and impurity levels (E_{imp}). The spectrum width ΔE of film is 0.2-0.3 eV less than that of matrix.

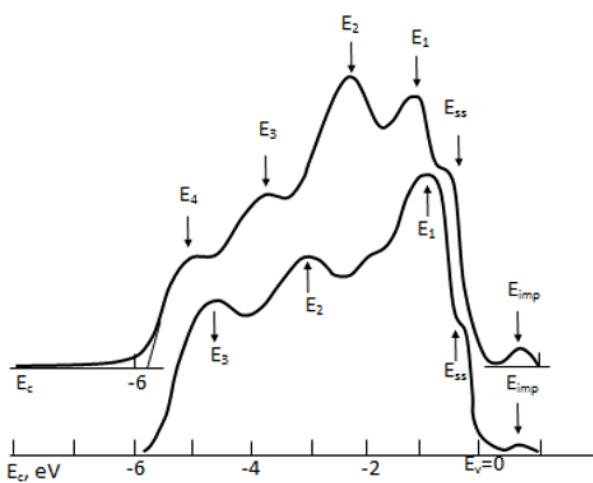


Fig. 1. The photoelectron spectra of pure CdTe (100) and with Cd_{0.6}Zn_{0.4}Te nanofilm for $h\nu=10.8$ eV.

The spectra $N(E_2)$ measured for $E_p=5$ eV for pure CdTe and for CdTe with a submonolayer Cs film ($\theta \approx 0.2$) are presented in Fig.2. E_2 is the energy of secondary electrons. Zero on the E_2 axis corresponds to a vacuum level of the CdTe film. From Fig. 3 it is seen that after Cs deposition the emission of true-secondary electrons into vacuum increases and the spectrum start sifts to lower energy by ~ 2.6 eV, i.e. the potential barrier (electron affinity χ) decreases by 2.6 eV. In this part of the spectrum there are peculiarities for energy $E_{c1}=-1$ and $E_{c2}=-1.9$ eV (relative to E_v for energy 3.5 and 4.4 eV). The positions of these peculiarities correspond to maximums of the density of electronic states in the conductivity band. By increasing the thickness of the Cs film up to 0.5-0.6 in the monolayer it is possible to decrease χ by $\sim 3-3.5$ eV. However, beginning with $\theta \sim 0.4-0.5$ of monolayers, in the spectrum there are peculiarities associated with the Cs atoms.

The dependences of true-secondary electrons δ , elastically reflected ones χ and dR/dE_p on primary electron energy E_p for CdTe(111) within the range of $E_p=0-20$ eV are presented in Fig.3. The peculiarities of the curve $R(E_p)$, i.e. maximums of the curves $dR/dE_p(E_p)$, correspond to the electron transitions from

the valence band maximums into the conductivity zone maximums [11]. Analysis of the $dR/dE_p(E_p)$ curve (spectra of elastically reflected electrons) for photoelectrons (Fig.1) and true-secondary electrons showed that the maximum E_1' corresponds to the electron transition from E_v to E_c (approximately equal to E_g); E_2' to the transition from E_1 to E_{c1} ; E_3' to the transition from E_v to E_2 ; and E_4' to the transition from E_2 to E_{c2} . The maximums E_6' and E_7' can be probably associated with the electron transition from the maximums of the density of the valent electron states into the maximum of free states in vacuum. The position E_3' corresponds to an initial immediate increase in δ , which is due to the electron transition from the top of the valent zone into vacuum. For $E_p=11.2$ eV there is also an immediate decrease in R (maximum on the curve dR/dE_1). However, for this energy E_p there is no immediate increase in δ . Owing to the above statements it is possible to suppose that the valence electrons move not to vacuum but to a maximum of the conductivity band. For the width of the forbidden band of CdTe to be defined more accurately, the energy dependence of the intensity I of light transmitting through CdTe was measured within the range $h\nu=0.6-2$ eV [10]. From Fig.4 it is seen that for CdTe E_g is ~ 1.45 eV.

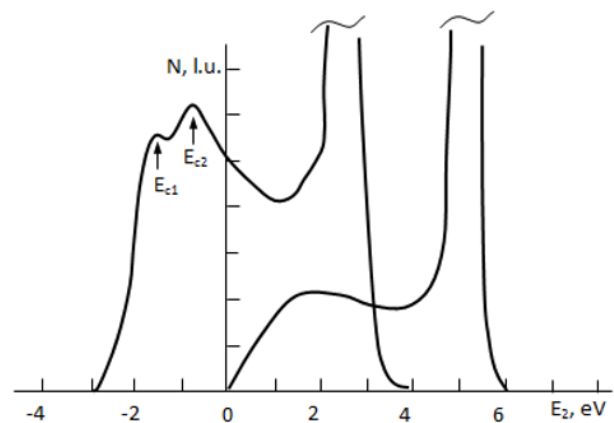


Fig. 2. The spectra $N(E_2)$ measured for $E_p=5$ eV for pure CdTe and CdTe with the submonolayer ($\theta \approx 0.2$) film of Cs.

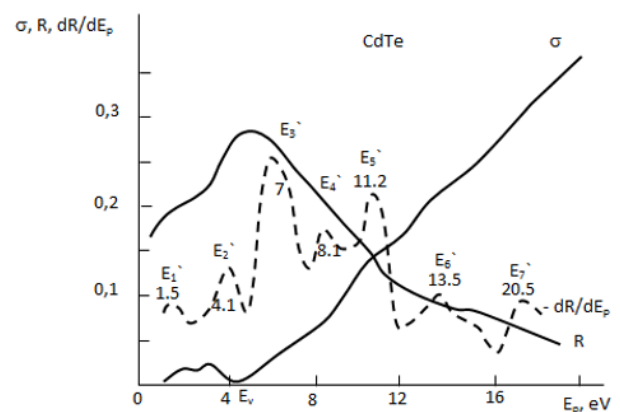


Fig. 3. The dependences of δ , R and dR/dE_p on energy of primary electrons for CdTe(111).

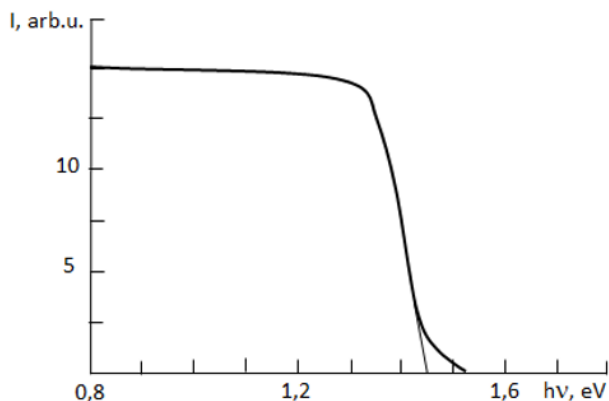


Fig. 4. The energy dependence of the intensity I of light transmitting through CdTe.

4 Conclusion

Thus, in this paper the nano-crystalline phases and nanofilms of CdBaTe and CdZnTe were formed and their band-energy parameters and the densities of occupied and free electronic states have been studied by the technique of low-energy ion implantation on the surface of single crystals CdTe(111).

References

- [1] C.H. Lee, S.W. Park, Lee Jaesun, Y.M. Moon, et al., *J. Electron. Mater.* **27**, 6, 668 (1998)
- [2] A.V. Brodovoy, S.G. Bunchuk, Z.F. Tcibriy, *FTT* **53**, 3, 524–526
- [3] P.N. Tkachuk, *FTT* **42**, 11, 1961–1963 (2000)
- [4] K.D. Glinchuk, A.P. Medvid, A.M. Mychko, et al., *FTP* **47**, 4, 435–441 (2013)
- [5] N.I. Klyuy, V.B. Lozinskiy, A.N. Lukyanov, V.A. Morojenko, R.K. Savkina, et al., *JTF* **82**, 8, 83–86 (2012)
- [6] M.K. Herndon, A. Gupta, V.I. Kaydanov, R.T. Collins, *Appl.Phys. Lett.* **75**, 3503 (1999)
- [7] S.A. Muzafarova, Sh.A. Mirsagatov, J. Janabergenov, *FTT* **49**, 6, 1111–1116 (2007)
- [8] B.E. Umirzakova, D.A. Tashmukhamedovab, M.K. Ruzibaevaa, F.G. Djurabekova, S.B. Danaev, *NuclearInstr.AndMehodsInPhys. Research Section B: Beam Inerac. WithMaterials and Atoms* **326**, 322–325 (2014)
- [9] Y.S. Ergashov, D.A. Tashmukhamedova, B.E. Umirzakov, *Journal of Surface Investigation* **11**, 2, 480–484 (2017)
- [10] Z.E. Mukhtarov, Z.A. Isakhanov, B.E. Umirzakov, T. Kodirov, E.S. Ergashev, *Technical Physics* **60**, 12, 1880–1884 (2015)